35th Annual International Conference of the IEEE EMBS
Osaka, Japan, 3 - 7 July, 2013

Needle-free Interstitial Fluid Acquisition Using a Lorentz-Force Actuated Jet Injector*

Jean H. Chang, N. Catherine Hogan, and Ian W. Hunter

Abstract— **The feasibility of a new method of quickly acquiring interstitial fluid (ISF) samples using a Lorentz-force actuated needle-free jet injector is demonstrated on ex vivo porcine tissue. The jet injector is used to first inject a small volume of physiological saline to breach the skin, and the back-drivability of the actuator is utilized to create a vacuum in the ampoule and collect ISF. Injection and extraction parameters are tested and optimized for minimal acquired sample dilution and extracted volume consistency. Using this method, we are able to collect a sample that contains up to 3.5% ISF in 3.1 s.**

I. Introduction

Interstitial fluid (ISF) samples can provide a great deal of information on a patient's health, as they contain regulatory molecules that are correlated with disease-related processes. It has been shown that glucose levels in dermal interstitial fluid are an indicator of blood glucose levels [1]. There has also been recent interest in proteomic characterization of tumor interstitial fluid, the fluid that perfuses the tumor microenvironment. Studies on the protein composition of tumor interstitial fluid can lead to a new resource for diagnostic biomarker discovery and the ability to identify more selective targets for cancer treatments [2]. Determining the composition of an ISF sample can therefore aid in early disease detection and in the evaluation of treatment efficacy.

There is currently a lack of minimally invasive ISF acquisition devices that are able to quickly collect samples. While improvements have been made in the past 15 years on older methods of sample acquisition (e.g. tissue excision [3], implantable wicks [4], or suction blister devices [5]), most devices are still invasive and involve the use of needles. Typical ISF extraction devices involve breaching the skin using a lancet or laser and then application of a vacuum for at least 10–20 minutes to collect the sample. Newer devices such as microneedle arrays, which employ capillary action to draw ISF, claim to reduce the amount of pain but can suffer from other problems such as tissue clogging [6]. Sonophoretic devices are noninvasive and do not require breaching the skin, but can only obtain ISF from shallow depths (epidermal ISF) [7], and are unable to collect larger items such as cells. All of these acquisition devices are slow due to the low permeability of the tissue matrix [8]. Slow acquisition methods not only can cause more discomfort for the patient, but also suffer from erroneous measurements since the application of a vacuum for tens of minutes may increase net capillary filtration, resulting in a lower interstitial fluid concentration [3]. Implantable continuous monitoring sensors do not require actual ISF extraction, but can yield inaccurate measurements due to inflammatory responses at the implantation site [9].

Here we demonstrate the feasibility of a minimally invasive technique for obtaining ISF samples using a needle-free jet injector. The needle-free jet injector (JI) developed at the BioInstrumentation Lab is a novel servo-controlled, Lorentz force actuated needle-free device that allows for precise control over penetration depth and injected volume [10–11]. The linear motor pressurizes the fluid contained in a drug ampoule and ejects it through a small (~200 μm) orifice, resulting in a narrow, high-speed (100–200 m/s) fluid jet with sufficient pressure to penetrate tissue.

The JI is used to first deliver a high-pressure jet of physiological saline to puncture the tissue (Fig. 1a). The high speed of the injectate allows for mixing with the interstitial fluid in the tissue (Fig. 1b). The bi-directionality of the Lorentz force actuator is then utilized to reverse the piston direction, creating a vacuum inside the ampoule. If the piston is reversed before the injectate fully disperses into the surrounding tissue, a high pressure differential is created between the injected area and the ampoule. This pressure differential allows for a mixture of the injectate and interstitial fluid to flow into the ampoule (Fig. 1c) in a much shorter period of time than with the simple application of a vacuum.

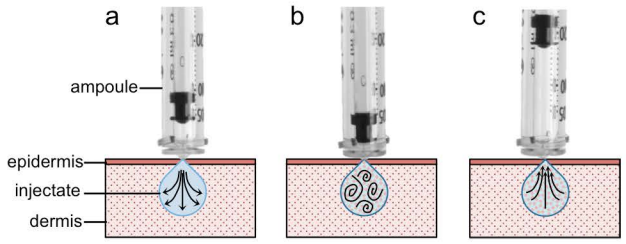

Figure 1. Schematic of extraction process. (a) Physiological saline is injected into the skin. (b) Injectate mixes with ISF. (c) Piston direction is reversed. The vacuum created in the ampoule along with the pressure increase in the tissue due to the injection allows for the sample to flow into the ampoule.

This technique offers advantages over other ISF acquisition devices in that it is able to obtain a fluid sample in a fraction of the time that other devices require, which can lead to more accurate measurements and increased patient compliance. Additionally, the lack of needles can result in a smaller puncture hole (i.e. less tissue damage) at the treatment site (a 27 gauge needle is 413 μm in diameter, while the fluid jet created by the jet injector can be designed to be 50–200 μm in diameter).

*This work was supported by Sanofi S.A., Paris, France.

J. H. Chang, N. C. Hogan, and I. W. Hunter are with the BioInstrumentation Laboratory, Department of Mechanical Engineering, Massachusetts Institute of Technology, Cambridge, MA 02139 USA (phone: 617-324-6052; fax: 617-252-1849; e-mail: jean_c [at] mit.edu).

II. Materials and Methods

A. Instrumentation

The jet injector device, shown in Fig. 2, was similar to a previously described MIT BioInstrumentation JI [11], and consists of a custom-made Lorentz-force motor, a very high energy density neodymium magnet, custom-built housing, a position sensor, and a commercially available drug ampoule (Injex Ampoule, part #100100). The housing was fixed onto an adjustable vertical linear stage. A tissue mounting stage included a load cell to measure the contact force that the JI applied to the tissue.

The control system used a compact reconfigurable input-output (cRIO) system comprising a real-time controller (cRIO-9024, National Instruments) embedded in a reconfigurable field-programmable gate array (FPGA) chassis (cRIO-9113). Replaceable I/O modules in the cRIO chassis provided analog as well as digital input and output channels. Two linear power amplifiers (AE Techron 7224) configured in series were used to amplify the analog control signal and drive the actuator.

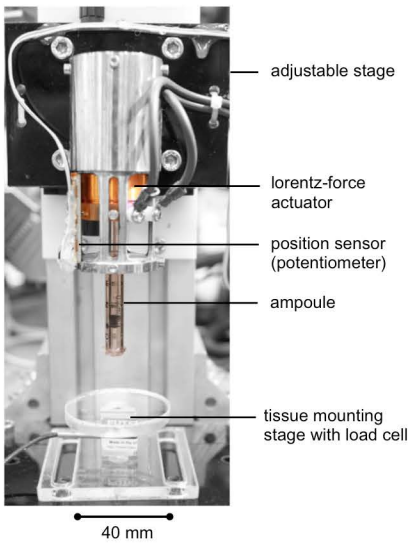

Figure 2. Benchtop version of Lorentz-force actuated jet injector.

B. Software

The injection control software was similar to that of a previously described MIT BioInstrumentation jet injector, and was written in LabVIEW 2011 [11]. Briefly, the injection controller consisted of a velocity feedforward controller that allowed for the motor to follow a preset waveform, and a proportional-integral-derivative (PID) motor position controller for stability, disturbance rejection, and delivered volume control. Injections were delivered using a two-phase waveform described in detail elsewhere [11]. A typical waveform is shown in Fig. 3a. The user sets the initial high speed (v_{jet}), time at high speed (t_{jet}), lower following speed (v_{follow}), and injection volume (Vol). A typical injection lasts tens of milliseconds. The reliability and accuracy of the device is described in [11].

An extraction module was added to the jet injector software. The extraction controller was a PID motor position controller. The user defines the wait time (t_{wait}) between the end of the injection phase and the beginning of the extraction phase. The user also defines the shape of the coil position versus time waveform. Two different waveform shapes were tested: a single-phase waveform (Fig. 3b) where the piston is retracted at a constant speed (v_{piston}) and a two-phase waveform (Fig. 3c), where the piston is first retracted at a higher speed (v_1) to establish the vacuum, and subsequently retracted at a lower speed (v_2) to slowly draw fluid into the ampoule. The duration of the extraction was several (2–4) seconds.

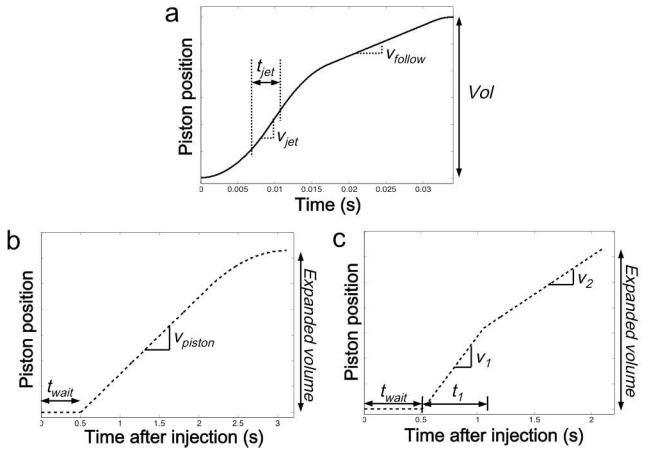

Figure 3. (a) Two-phase waveform used for injection. (b) Single-phase extraction waveform: the piston is retracted at a constant speed v_{piston} after a set t_{wait}. (c) Two-phase waveform used for extraction: the piston is retracted at v_1 to establish the vacuum, then slowed to v_2 to slowly draw fluid into the ampoule.

C. Injection Protocol

Post-mortem porcine tissue was obtained through the MIT Tissue Harvest Program using procedures approved by the MIT Committee on Animal Care and in accordance with the NIH Guide for the Use and Care of Laboratory Animals. Tissue was harvested from the abdomen of Yorkshire pigs approximately six months in age immediately after euthanasia and included muscle, subcutaneous fat, dermis, and epidermis. The samples were vacuum-sealed and stored at -80°C. Prior to experimentation, the samples were thawed to room temperature, and the skin surfaces were carefully cleaned with water.

Undiluted ISF samples were obtained by excising a portion of the dermis from the sample batch and centrifuging the fluid out of the tissue. Surface contamination samples were also collected to ensure that the analytes detected in the extracted fluid samples were from within the tissue and not from the skin surface. Surface contamination samples were collected by placing 20 µL of sterile saline on the surface of the skin of each tissue sample.

For each extraction, the JI applied a contact force of 0.8 N onto the skin. The JI injected the tissue with a preset waveform (Fig. 3a), waited for a set period of time (t_{wait}), and then extracted a mixture of the injectate and ISF with a preset extraction waveform (Figs. 3b-c). Injection and extraction parameters were tested to determine their effects on extracted volumes and concentrations. Protein and glucose concentrations of each collected sample were quantified using a NanoOrange® Protein Quantitation Kit (Life Science

Technologies™) and an Amplex® Red Glucose/Glucose Oxidase Assay Kit (Life Science Technologies™). Acquired ISF sample concentrations were compared to surface contamination samples, and an extraction was deemed to be successful if the analyte concentration of the extracted sample was greater than the analyte concentration of the surface contamination sample. For comparison between trials, analyte concentrations were normalized by the respective protein and glucose concentrations in the undiluted ISF samples. The volumes of the extracted samples were also measured. Data sets were compared using the two tail *t*-test for unequal variances.

III. Results

A. Dependence on Injection Parameters

For Trials A–D, the injection parameters v_{jet} and Vol were varied while t_{jet} and v_{follow} were unchanged (t_{jet} = 2 ms and v_{follow} = 50 m/s). The extraction parameters were kept constant between trials; the piston was retracted using the single-phase waveform shown in Fig. 3b with v_{piston} = 10 mm/s, to a travel length of 21 mm (corresponding to a volume expansion of 210 mm^3), with a wait time of 400 ms. The extracted volumes and concentrations were measured and the results are shown in Fig. 4. A list of the injection parameters tested is shown in Table I.

TABLE I. Injection Parameters

Trial	v_{jet} (m/s)	Vol (µL)
A	150	50
B	175	50
C	150	100
D	175	100

The following injection parameters were the same across Trials A–D: t_{jet} = 2 ms; v_{follow} = 50 m/s. Extraction parameters across Trials A–D were: single-phase extraction waveform; t_{wait} = 400 ms; v_{piston} = 10 mm/s; expanded volume = 210 mm^3.

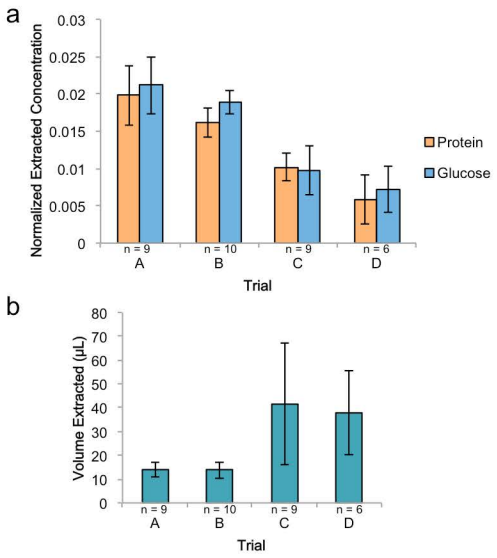

Figure 4. Results of trials where the injection parameters were varied. (a) Mean extracted protein and glucose concentrations, normalized by the concentration in undiluted ISF. Error bars represent standard errors. (b) Mean extracted volumes. Error bars represent standard deviations.

Injecting with 50 µL (Trials A and B) rather than 100 µL (Trials C and D) yielded higher extracted protein and glucose concentrations due to less dilution from the injectate. Injecting with 50 µL also resulted in much lower variability in the extracted volumes.

There was no significant difference in extracted volumes (p = 0.82) and concentrations (p = 0.52 for protein, p = 0.72 for glucose) between Trials A and B. However, it has been previously reported that the magnitude of v_{jet} will establish the injection depth [11–14]. We observed that the injectate stayed within the dermis and shallow subcutaneous layer for 50 µL injections performed with v_{jet} = 150 m/s, while the injectate reached deeper into the subcutaneous layer and even to the muscle when v_{jet} = 175 m/s. A v_{jet} of 150 m/s was deemed to be more appropriate than v_{jet} = 175 m/s, since the target acquisition site is the dermis.

Thus, the optimal injection parameters were determined to be that of Trial A: v_{jet} = 150 m/s, t_{jet} = 2 ms, v_{follow} = 50 m/s, and Vol = 50 µL.

B. Dependence on Extraction Parameters

Trials E–G investigated the effects of the extraction waveform. The optimal injection parameters of Trial A were used: v_{jet} = 150 m/s, t_{jet} = 2 ms, v_{follow} = 50 m/s, and Vol = 50 µL. Results are shown in Fig. 5. A list of extraction parameters tested is shown in Table II.

TABLE II. Extraction Parameters

Trial	Waveform type	Waveform parameters	Wait time (ms)	Extraction time (s)
A	Single-phase	v_{piston} = 10 mm/s	400	2.7
E	Single-phase	v_{piston} = 5 mm/s	400	4.3
F	Single-phase	v_{piston} = 10 mm/s	80	2.5
G	Two-phase	v_1 = 10 mm/s; v_2 = 5 mm/s; t_1 = 1000 ms	80	3.1

The following injection parameters were the same for Trials A, E – F: v_{jet} = 150 m/s; t_{jet} = 2 ms; v_{follow} = 50 m/s; Vol = 50 µL. The total volume expansion for extraction was 210 mm^3.

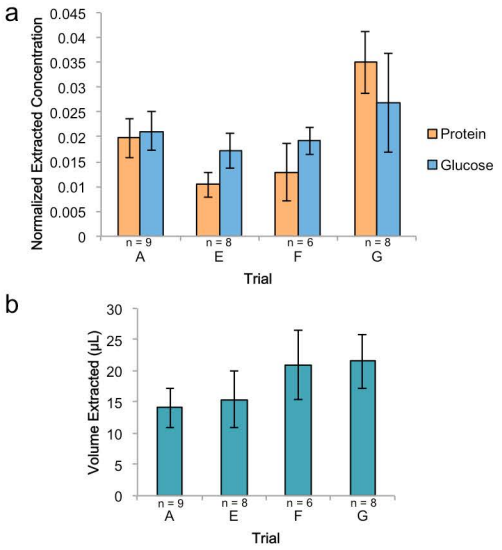

Figure 5. Results of trials where the extraction parameters were varied. (a) Mean extracted protein and glucose concentrations, normalized by the concentration in undiluted ISF. Error bars represent standard errors. (b) Mean extracted volumes. Error bars represent standard deviations.

For the single-phase waveform, extracting with v_{piston} = 10 mm/s (Trial A) recovered significantly more protein (p =

0.05) than when v_{piston} = 5 mm/s (Trial E). There was no statistical significance for the recovered glucose concentrations (p = 0.4). There was also no statistical difference in the extracted protein (p = 0.2) and glucose (p = 0.8) concentrations for a shorter t_{wait} (Trial A vs. Trial F). A shorter t_{wait} however resulted in higher overall volume recovery (p = 0.03). Thus, although the concentrations of the analytes in the extracted sample remained unchanged between the two trials, the overall amount of analytes was greater for Trial F due to the larger recovered volumes. A short t_{wait} is advantageous for applications such as proteomic characterization, where the presence of certain biomarkers is of interest rather than the actual concentration of such analytes.

Trial G used the two-phase extraction waveform shown in Fig. 3c. The purpose of the two phases was to first quickly establish a seal between the skin and the ampoule, and then draw the fluid slowly into the ampoule. The data show a vast improvement in both the consistency of the volume extracted and the recovered protein concentration when using the two-phase waveform. When compared to the best of the single-phase waveform trials (Trials A and F), extraction with the two-phase waveform resulted in significantly more protein recovery (p = 0.04 when compared to Trial A and p = 0.01 when compared to Trial F). Additionally, Trial G had a higher volume recovery than Trial A (p = 0.002). While Trial G had extracted volumes comparable to Trial F, Trial G had a smaller standard deviation and therefore more consistent extracted volumes.

Thus, a two-phase extraction waveform recovered more ISF than a simple, single-phase waveform. We hypothesize that the quick establishment of the seal in the first phase results in less air leakage. Further experimentation will optimize the parameters for this extraction waveform.

IV. Conclusion

We demonstrate the feasibility of using a needle-free jet injector for the acquisition of interstitial fluid. This work establishes that the injection parameters as well as the extraction waveform shape will affect the amount of ISF acquired. A two-phase extraction waveform showed better results than a simple, single-phase extraction waveform.

To the best of the authors' knowledge, this is the first time that such a technique for ISF acquisition has been attempted. While the sample is diluted, most assays are sensitive enough to detect the quantities obtained in our samples. Additionally, there are a number of advantages for injecting first with physiological saline—the most notable advantage being time. The device can also be optimized for the extraction of other fluids such as tumor ISF, spinal fluid, and blood. Furthermore, the method can be developed for applications such as tissue biopsies or whole cell extractions, where sample dilution is not an issue.

Since the time constant of the extraction process is on the order of seconds, this method offers advantages over slower ISF acquisition methods. Notably, the short duration of the acquisition allows for a measurement that is representative of a moment in time, rather than averaged over tens of minutes. Additionally, since the time constant of diffusion is on the order of minutes, there is not enough time for the body to equalize the imbalance caused by the injection of saline, nor is there enough time to produce an inflammatory response.

Future work may include development of a theoretical model that can predict the extent of dilution in the acquired sample. Additional experimentation to determine the optimal parameters for minimal dilution of ISF will be performed. Live animal studies will also be performed to determine the effects of interstitial pressure on the acquisition process. It is well known that the dermal interstitial pressure is slightly below ambient pressure [15] while tumor interstitial pressure is slightly above ambient pressure [16].

Acknowledgment

The authors would like to thank Adam J. Wahab for his help with the device hardware and software setup.

References

[1] J. P. Bantle and W. Thomas, "Glucose measurement in patients with diabetes mellitus with dermal interstitial fluid," *J. Lab. Clin. Med.*, vol. 130, pp. 436–441, 1997.

[2] J. E. Celis, P. Gromov, T. Cabezón, J. M. A. Moreira, N. Ambartsumian, K. Sandelin, F. Rank, and I. Gromova, "Proteomic characterization of the interstitial fluid perfusing the breast tumor microenvironment," *Mol. Cell. Proteomics*, vol. 3, pp. 327–344, 2004.

[3] R. K. Jain, "Transport of molecules in the tumor interstitium: A review," *Cancer Res.*, vol. 47, pp. 3039–3051, 1987.

[4] H. O. Fadnes, R. K. Reed, and K. Aukland, "Interstitial fluid pressure in rats measured with a modified wick technique," *Microvasc. Res.*, vol. 14, pp. 27–36, 1977.

[5] U. Kiistala, "Suction blister device for separation of viable epidermis from dermis," *J. Invest. Dermatol.*, vol. 50, pp. 129–137, 1968.

[6] W. Martanto, J. S. Moore, T. Couse, and M. R. Prausnitz, "Mechanism of fluid infusion during microneedle insertion and retraction," *J. Control. Release*, vol. 112, pp. 357–361, 2006.

[7] S. Mitragotri, M. Coleman, J. Kost, and R. Langer, "Analysis of ultrasonically extracted interstitial fluid as a predictor of blood glucose levels," *J. Appl. Phys.*, vol. 89, pp. 961–966, 2000.

[8] J. R. Levick, "Flow through interstitium and other fibrous matrices," *Exp. Physiol.*, vol. 72, pp. 409–437, 1987.

[9] E. Cengiz and W. V. Tamborlane, "A tale of two compartments: interstitial versus blood glucose monitoring," *Diabetes Technol. Ther.*, vol. 11, supp. 1, pp. S-11–S-16, 2009.

[10] I. W. Hunter, A. J. Taberner, B. D. Hemond, D. M. Wendell, N. C. Hogan, N. B. Ball. Controlled needle-free transport. US2007191758-A1; US7833189-B2.

[11] A. J. Taberner, N. C. Hogan, and I. W. Hunter, "Needle-free jet injection using real-time controlled linear Lorentz-force actuators," *Med. Eng. Phys.*, vol. 10, pp. 1–8, December 2011.

[12] B. D. Hemond, A. Taberner, N. C. Hogan, B. Crane, and I. W. Hunter, "Development and performance of a controllable autoloading needle-free jet injector," *J. Med. Devices*, vol. 5, pp. 1–7, 2011.

[13] D. M. Wendell, B. D. Hemond, N. C. Hogan, A. J. Taberner, and I. W. Hunter, "The effect of jet injection parameters on jet injection," in *Conf. Proc. IEEE Eng. Med. Biol. Soc.,* vols. 1–15, pp. 2668–2671, 2006.

[14] J. C. Stachowiak, T. H. Li, A. Arora, S. Mitragotri, and D. A. Fletcher, "Dynamic control of needle-free jet injection," *J. Control. Release*, vol. 135, pp. 104–112, 2009.

[15] P. F. Scholander, A. R. Hargens, and S. L. Miller, "Negative pressure in the interstitial fluid of animals," *Science*, vol. 161, pp. 321–322+325–328, 1968.

[16] C.-H. Heldin, K. Rubin, K. Pietras, and A. Ostman, "High interstitial fluid pressure—an obstacle in cancer therapy," *Nature Reviews Cancer*, vol. 4, pp. 806-813, 2004.